[Supplementary material]

Early to Middle Bronze Age agricultural terraces in north-east England: morphology, dating and cultural implications

Antony G. Brown[1,2,*], Daniel Fallu[1], Sara Cucchiaro[3], Monica Alonso[4,5], Rosa Maria Albert[4,5,6], Kevin Walsh[7], Ben R. Pears[2], Rob Scaife[2], Catherine Langdon[2], Paolo Tarolli[3], David Cockroft[8], Lisa Snape[9], Andreas Lang[9], Philippa Ascough[10], Pengzhi Zhao[11], Kristof Oost[11] & Clive Waddington[8]

[1] Natural Sciences, Tromsø University Museum, Arctic University of Tromsø, Norway

[2] Geography & Environmental Science, University of Southampton, UK

[3] Department of Land, Environment, Agriculture and Forestry, University of Padova, Italy

[4] Multidisciplinary Research Institute (MARI); Vrije Universiteit Brussel, Belgium

[5] ICREA, Barcelona, Spain

[6] Department of Prehistory, Autonomous University of Barcelona, Spain

[7] Department of Archaeology, University of York, UK

[8] ARS Ltd, Bakewell, UK

[9] Geography & Geology, University of Salzburg, Austria

[10] NEIF Radiocarbon Laboratory, SUERC, Glasgow, Scotland

[11] Georges Lemaître Centre for Earth and Climate Research, Earth and Life Institute, UC Louvain, Louvain-la-Neuve, Belgium

[*] Author for correspondence ✉ antony.g.brown@uit.no

OSM1: stratigraphic recording

The trench was recorded using standard archaeological procedures, i.e. recognition of uniform units separated by discontinuities, which were given context numbers. In addition, sampling profiles were described using standard UK soils notation based on the properties of horizons and the identification and description of discontinuities between horizons (Hodgson 1976). When not buried under sediment rather than soil, the soil horizons are denoted using only the standard characteristics and not their position in the profile. This means that burial is not included as a criterion, and so is not added as a prefix (alphanumerical or numerical), as it is in the Soil Conservation System in the USA (Bettis 1984). In the Food and Agriculture Organization of the United Nations (2006) system, there is a specific designation of a buried B horizon but it is placed as a subscript rather than a prefix. The sub-division of B horizons

follows changes in stoniness and matrix colour, which are also generally reflected in the archaeological context boundaries. As these are fundamentally young cumulative and ploughed soils, these two systems probably provide similar stratigraphy due to a lack of weathering and pedological overprinting. The differentiation between A, B and C horizons followed standard soils criteria and the separation of multiple B horizons was caused by slight variations in stoniness and colour (e.g. B2d for a denser lower B horizon). Ap horizons were identified on higher organic matter than B horizons but with an open matrix supported, relatively isotropic structure with a sharp lower boundary. The two control pits showed incipient podzolisation of the upper B horizons not visible in the trench profiles. For a description of soil horizon notation as used here, refer to Hodgson (1976).

OSM2: pOSL

Luminescence readings were taken using a SUERC portable optically stimulated luminescence reader (Sanderson & Murphy 2010). Samples for portable optically stimulated luminescence were taken in bulk using plastic bags held within a light proof black bag. Samples of roughly 25g were measured for a total of 60 seconds under infrared light and 60 seconds under blue light. Soil Profiles (Tp) 2 and 3 were run under semi/field conditions in the field accommodation in Northumberland using a custom protocol (15 seconds dark, 60 seconds infrared, 60 seconds blue light and 15 seconds dark). The remaining samples (Soil Profiles (Tp) 1 and 4) were processed in darkroom conditions back at the Tromsø Museum botany station using the SUERC CW protocol (dark 15 seconds, infrared 30 seconds, infrared 30 seconds dark 15 seconds, blue light 30 seconds, blue light 30 seconds, dark 15 seconds). OSL intensity was calculated for each sample following Sanderson & Murphy (2010). In order to compare the results, the values were divided by the intensity of the closest-to-surface sample in their respective profile, generating a representation of the intensity as a factor of the intensity of the most recently deposited/exposed sediment. The resulting index of relative OSL intensity was used to relate and interpret the lithostratigraphy and soil horizonation with the radiocarbon dates from Soil Profile 1 (Tp 1 4 and Tp 1 22). The histogram, at eight bins, shows 17 pOSL intensities in the same range as Tp1 1.22 (7.625406–14.43176) corresponding to a photon count range of 1.35872 × 105–2.37307 × 105 in the SP 1 intensity readings. This range is identified in the buried soil, occurring in the Ap or B1 horizons identified by excavators.

OSM3: pXRF

Portable X-Ray fluorescence (pXRF) was used for general characterisation of the sediments, namely, to identify elemental concentrations that may be related to rapid burial associated with the installation of terraces or the weathering of the established soils. Scans were performed with an Olympus Vanta M Series pXRF Analyser (Rhodium source 8–50kV, 3mm diameter beam spot). Preliminary scans were conducted with 15ml sample jars with a cap modified to hold a polypropylene film for x-ray analysis. Each sample was disaggregated and homogenised for five minutes using a borosilicate glass mortar and pestle. The homogenised sample was then placed into the sample jar with the modified cover, which was then placed film side down onto the aperture of the pXRF scanner in bench mode and tapped so that the sediment settled against the film as much as possible. Each sample was scanned three times on two settings: 'Soil' and 'Geochemistry'. Each setting was run at its factory set length to ensure quick scans. Scanning with the Vanta M series took advantage of the high count rates and spectrum resolution for relatively high accuracy for low scan times, in this case the factory settings (Frahm 2017). The 'Soil' setting was run for a total of 50 seconds (10s at 50kV, 20s at 40kV and 20s at 15kV), while the 'Geochemistry' setting was run for 30 seconds (10s at 40kV and 20s at 10kV). Results from the three runs on each mode were averaged in ppm. Results presented in this study are from the 'Geochemistry' setting and are uncalibrated. Few studies have analysed terrace soils using this approach but the framework for interpretation is provided by Brown *et al*. (2021) and weathering indices have been computed for agricultural soils (e.g. Gozukara 2022).

OSM4: HyPy-PyC AMS radiocarbon dating

Hydropyrolysis (HyPy) dates the most resistant organic fraction of the soil (black or pyrogenic carbon (BC/PyC) through a process of reductive removal of non-BC components, and so is less susceptible to contamination and intrusion (Ascough *et al.* 2020). PyC, as defined by HyPy, consists of polycyclic aromatic carbon greater than or equal to seven aromatic rings (Ascough *et al*. 2009; Meredith *et al*. 2012). The process reductively separates and isolates these structures in a mixed sample (e.g. soil, sediment). Ground and dried soil samples were first decarbonised by digestion in 1M HCl (80°C for two hours) before neutralising with Milli-Q® water. Samples were then loaded with the HyPy catalyst at 5% by weight (nominal loading of 0.5% Mo) using an aqueous/methanol (1:1) solution of ammonium dioxydithiomolybdate [$(NH_4)_2MoO_2S_2$]. Catalyst-loaded samples were pyrolysed at 550°C under a hydrogen pressure of 150 bar and sweep gas flow of 5Lmin^{-1}(ATP). Following HyPy, the solid residue containing PyC was converted to CO_2 by combustion with

CuO and Ag in a sealed quartz tube. Following cryogenic purification, sample CO_2 was converted to graphite by Fe/Zn reduction for subsequent radiocarbon measurement by accelerator mass spectrometry. Note that, for the HyPy dates, the laboratory $\delta^{13}C$ values, although appropriate to correct ^{14}C values for isotopic fractionation, are not necessarily representative of the $\delta^{13}C$ in the original sample material, and so these values are therefore not suitable for purposes other than ^{14}C data normalisation and are not reported in Table 1 to avoid confusion. All samples from ^{14}C assay were calibrated in CALIB 8.2 using the IntCal20 (Reimer *et al*. 2020; Stuiver *et al*. 2022).

OSM5: pollen and spores

Due to low concentrations, large samples were used (1–2ml) and illustrated by swirling prior to sieving, followed by standard extraction methods involving acetolysis and hydrofluoric acid digestion, the addition of an exotic marker (Lycopodium) and mounting in glycerine gel. Standard keys were used for identification along with the reference collections at the University of Southampton. A sum of at least 350 total land pollen (TLP) was generally achieved except for one sample which only reached 270. The volumes and raw data are presented in Table S1.

Cereal type identification

In the sub-fossil state, the detailed identification of pollen of cereal type to a lower taxonomic level is frequently not feasible. Here, cereal pollen comprised *Avena, Triticum* and *Hordeum* types (Dickson 1988). The often-cited size criterion of pollen of >45u (depending on glycerol/silicone oil mountant; Moore *et al*. 1991: 100) is not reliable, as typically some pollen grains fall below this size delimitation. A number of pollen 'keys' and published descriptions are available to aid identification of cereal pollen and separation into taxonomic groups (Faegri & Iversen 1975; Andersen 1979; Dickson 1988; Moore *et al*. 1991; Beug 2004). For this article, cereal identification is based on typically more robust pollen grains; that is, those with thicker exine (which thus stains darker), a visible and organised columellate structure and frequently (but not always) large pore/annulus. A comparative collection and phase microscopy were available. These attributes very clearly differentiated cereal pollen from large pollen typically originating from a number of wild taxa. These include *Ammophila arhenaria, Spartina anglica* and especially *Glyceria fluitans*, which, apart from their size, are of the same character of typical wild/non cultivated grasses. *Secale cereale* did not present a problem with distinctive annulus and shape. It is also highly

unlikely, given the non-saline, inland and dry nature of the site, that that any of these three species were growing on in the vicinity.

OSM6: organic matter

In order to determine organic matter content of each horizon, 60g of 5mm sieved air-dried soils were analysed for total carbon and nitrogen using a VarioMax CN Element Analyzer (Elementar GmbH, Germany). Samples were also fractionated in order to determine the relative protection of the soil carbon in order to quantify the carbon storage in the terraces, and the results of this analysis can be found in Zhao *et al.* (2021).

OSM7: phytoliths and assessment of burning

Phytoliths, which have been shown to have high potential, at least from urban deposits, in northern England (McParland 2016), were sampled from individual horizons to avoid problems associated with bulked samples (Wade *et al*. 2019). Twenty-six samples were collected for phytolith analyses at four points within the trench cut into the terrace system at Plantation Camp: Tp1 (n = 4), T2 (n = 9), Tp3 (n = 8) and Tp4 (n = 8) (Figure 3). Samples were collected from bottom to top with a range of about 0.20–0.25m between samples. Phytolith extraction was carried out following Katz and colleagues (2010). Between 20 and 50mg of sediment were placed in a 0.5ml Eppendorf tube and 50µl of HCl 6N were added in order to remove carbonates. After the reaction disappears, 450µl of sodium polytungstate solution [$Na_6(H_2W_{12}O_{40})H_2O$] with a density of 2.4g/ml was added. The tube was vortexed and sonicated for 10 minutes, and then centrifuged for five minutes at 5000 rpm to separate phytoliths from clays. The supernatant was removed and transferred to another tube. A total of 50µl of the aliquot was placed on a microscope slide and covered with a 24 × 24mm coverslip. Phytoliths present in 20 visual fields at 200× magnification were counted for phytolith quantification. Morphological identification was based on our own modern reference collection (Albert *et al*. 2016; www.phytcore.org) as well as standard literature (Twiss *et al*. 1969; Brown 1984; Mulholland & Rapp 1992; Twiss 1992; Piperno 2006). Morphological descriptions follow the new international code for phytolith nomenclature (International Committee for Phytolith Taxonomy 2019).

In order to assess potential burning of the soils, ash pseudomorphs extraction was carried out following Gur-Arieh and colleagues (2013). Between 30 and 40mg of dried sediments are sieved through a 150µm sieve in order to remove particles greater than 150µm. After that, 500µl of sodium polytungstate solution [$Na_6(H_2W_{12}O_{40})H_2O$] with a density of 2.4g/ml is

added, and the sample sonicated for 10 minutes in order to disaggregate all the elements. Then, 50µl of the solution are placed on a microscope slide and covered with a 24 × 24mm coverslip. Micro-remains were identified under polarised light at 400× magnifications. Fourier-transformed infrared spectra (FTIR) analyses are carried out following the same method as Weiner and colleagues (1993): tens of micrograms of the archaeological sediment are homogenised with KBr in order to obtain pellets. Infrared spectra are obtained using a Nicolet iS5 spectrometer at $4cm^{-1}$ resolution. In addition, the reference collection provided by the Kimmel Center of Archaeological Science, Weizmann Institute of Science was consulted (http://www.weizmann.ac.il/kimmel-arch/infrared-spectra-library).
In order to identify whether phytoliths underwent burning processes, the refractive index (RI) of the phytoliths was checked according to Elbaum *et al*. (2003). Slides were prepared using Cargille medium with a refractive index of 1.440.

Further comments on the phytolith analysis and burning

Of the 26 samples analysed for phytoliths, 20 presented enough individual recognisable morphotypes for morphological interpretation (Albert & Weiner 2001). We calculated the amount of phytoliths per gram of sediment with the aim of comparing phytolith abundance in the samples. In general, the results indicate that the highest concentrations of phytoliths were in the intermediate samples, while the deeper samples presented very low concentrations, suggesting some degradation (Figure 5). Morphologically, the phytolith assemblage was dominated by the Poaceae family, with an emphasis on the C_3 Pooid subfamily. This group includes cereal grains of high economic importance, such as wheat and barley (Zohary *et al*. 2012). Most of the phytoliths corresponded to the leaves stems of these plants (as per TRAPEZOID, CRENATE) rather than the inflorescences (as per ELONGATE DENDRITICS) (Table S3). Phytoliths from the Cyperaceae family were also recovered from T3. Phytoliths from dicotyledonous plants were present in lower amounts and were mostly represented by BLOCKY. The results of the principal components analysis (Figure S4) show three different groups and three outliers that grossly coincide with the sample provenience in the trenches. Group A, characterised by having a high percentage of TRAPEZOID, integrates intermediate samples with highest phytolith concentration. No samples from T1 (Tp1) were included in this group. Group B is related to a higher presence of CRENATE and RONDEL, together with BLOCKY, the latter characteristic of dicot plants. Samples from this group were located both above and below previous group and presented lower phytolith abundance. No samples from T4 fall within this group. Group C presents a higher presence of BLOCKY,

and samples corresponding to this group (T1.2 and T4.5) were also located in upper and lower samples of the section. These samples have also low amounts of phytoliths per gram of sediment. Samples T3.5, T4.4 and T4.7 are outliers and do not relate amongst them (Figure S5). These differences in phytolith concentration and phytolith assemblage may indicate either change on cultivars or periodic abandonment of the terraces, that would be represented by samples with lower phytolith concentrations.

The different tests carried out on the phytoliths and related sediments did not show any evidence of burning. Neither the colour of the phytoliths nor the thermal alteration of silica was noted in the different morphotypes analysed. The refractive index of the phytoliths was also negative. In addition, microscopic observation of samples before chemical extraction did not show either the presence of micro-remains associated to burning processes, such as ash pseudomorphs, or siliceous aggregates. Finally, the FTIR did not show either indication of burning in any of the samples.

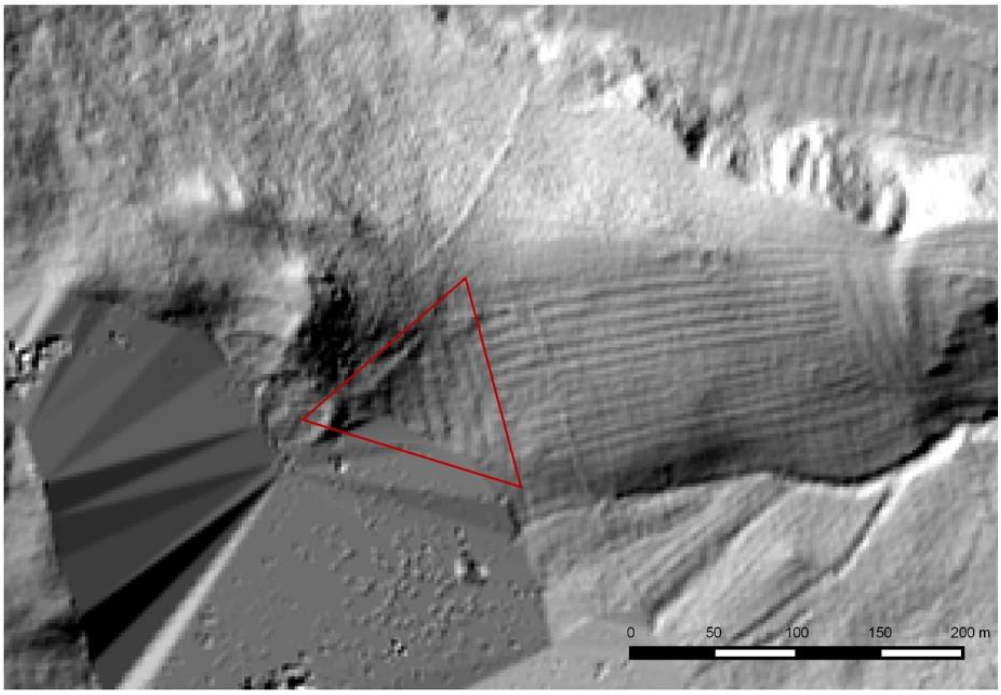

Figure S1. Digital elevation model (DEM) of Plantation Camp terraces (outlined in red) generated from the 2m Environment Agency Data flown in 2017 (data from DEFRA under Open Government License v3.0 https://environment.data.gov.uk/DefraDataDownload/?Mode=survey) (figure by C. Waddington/ARS Ltd).

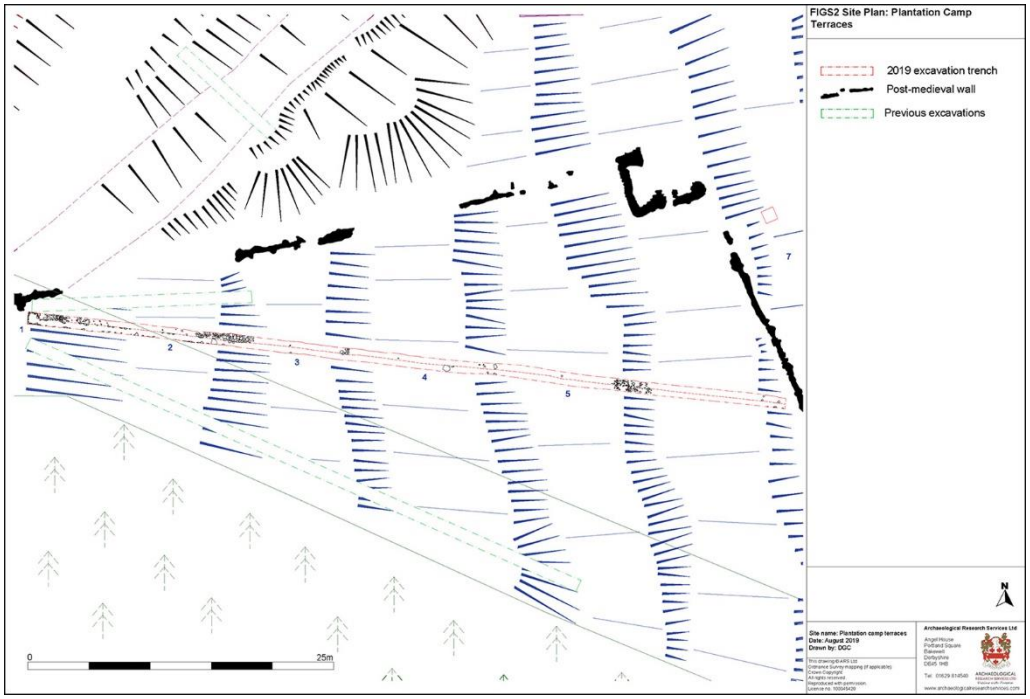

Figure S2. Earthworks survey of all excavations (adapted from Archaeological Services, University of Durham (2000) and the UAV-SfM HRT survey; figure by C Waddington/ARS Ltd).

Figure S3. Photograph of control pit TP2 showing a thin A horizon and single B horizon over clast rich C horizon material. The taught string length is 0.60m and pit depth is 1m (photograph by A.G. Brown).

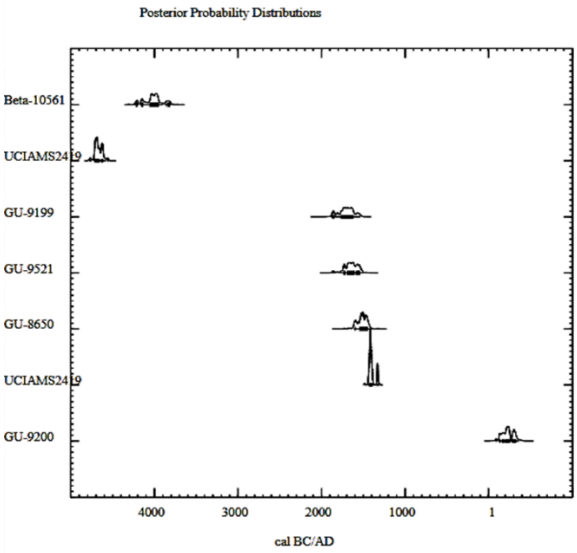

Figure S4. Dates posterior probability multiplot generated in CALIB 8.2 (Stuiver et al. *2022) using the IntCal20 curve (Reimer* et al. *2020) (figure by A.G. Brown).*

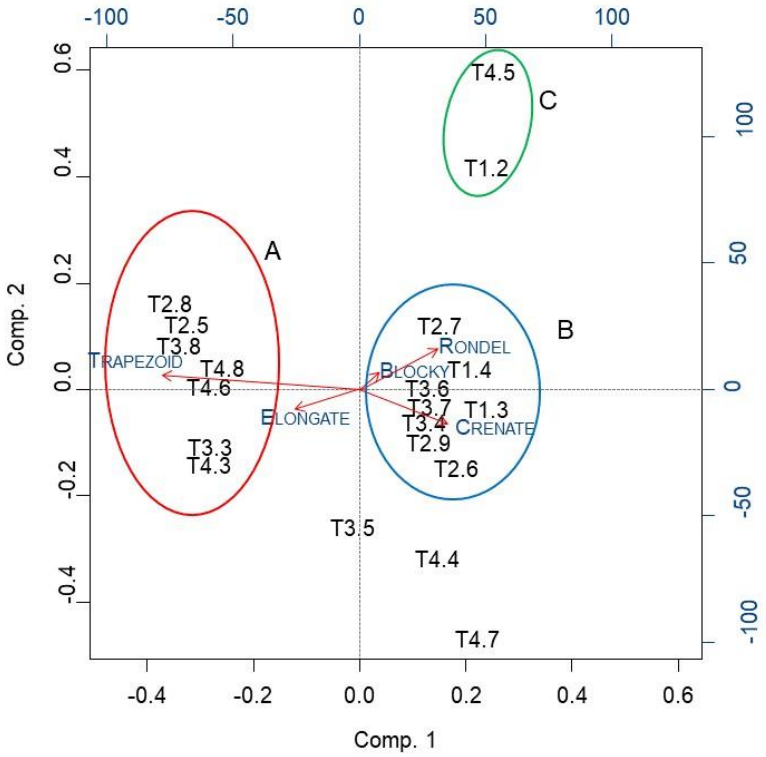

Figure S5. Principal component analysis of the morphotype composition of the samples, showing that there are three different groups according with the distribution of the morphotypes identified. Additionally, five morphotypes present high variability in the

sequences: TRAPEZOID, ELONGATE ENTIRE, RONDEL, BLOCKY and CRENATE (figure by M. Alonso).

Table S1. Soil horizons, pH and texture data.

Profile, horizon	**depth/m**	**pH**	**sand%**	**silt%**	**clay%**
Control TP4 (C1 in Zhao *et al*. 2021), A horizon	0–0.10	3.42	35.3	56.04	8.66
Control TP4 (C1 in Zhao *et al*. 2021), B horizon	0.30–0.45	3.9	43.5	44.6	11.9
Control TP4 (C1 in Zhao *et al*. 2021), C horizon	0.60–0.70	3.97	44.2	43.4	12.4
Control TP1 (C2 in Zhao *et al*. 2021), A horizon	0–0.10	3.13	58.2	39.6	2.74
Control TP1 (C2 in Zhao *et al*. 2021)	0.30–0.45	3.77	48.3	42.21	9.49
Terrace Tp1, Turf/topsoil	0–0.10	3.42	31.2	61.3	7.5
Terrace Tp1, Ap horizon	0.50–0.70	3.81	26.8	58	15.2
Terrace Tp1, B2 horizon	0.90–1.00	3.83	43	42.1	14.9
Terrace Tp1, C horizon	1.40–1.50	3.97	54.4	34.7	10.9
Terrace Tp2, Turf/topsoil	0–0.10	3.49	42.7	50.15	7.15
Terrace Tp2, Ap horizon	0.30–0.45	3.73	34.7	51.3	14
Terrace Tp2, B1 horizon	0.60–0.70	3.72	32.5	50	17.5
Terrace Tp2, B2 horizon	0.80–0.90	3.86	52.2	37.5	10.3
Terrace Tp3, Turf/topsoil	0–0.10	2.97	30.5	59.62	9.88
Terrace Tp3, Ap	0.30–0.45	3.78	35.5	50.9	13.6
Terrace Tp3, B1 horizon	0.60–0.70	3.94	47.5	41.4	11.1
Terrace Tp4, Turf/topsoil	0–0.10	3.35	39.9	51.58	8.52
Terrace Tp4, Ap	0.30–0.45	4.06	38.7	46.9	14.4
Terrace Tp4, B1 horizon	0.60–0.70	4.42	37.3	47.7	15

Table S2. Pollen data (Tp1, Tp4) (see Excel file).

Table S3. List of the average percentage of phytolith morphotypes identified in all samples, as well as their taxonomic/anatomical correspondence (following Neumann *et al*. 2019).

Morphotype	**Taxonomic/anatomic correspondence**	**% Average in phytolith record**
CRENATE	C_3 Grass leaves	26.81
TRAPEZOID	C_3 GSSCP	22.97
ELONGATE ENTIRE	Elongate	16.87
RONDEL	C_3 GSSCP	13.72
BLOCKY	Dicots wood/bark	7.78
BILOBATE	C_4 GSSCP	3.05
ACUTE BULBOSUS	Grasses leaves/stems	2.67
ELONGATE DENDRITIC	Grass inflorescences	1.05
BULLIFORM FLABELLATE	Grass leaves/stems	0.95
ELONGATE DENTATE	Grass inflorescences	0.93
SPHEROID PSILATE	Dicots wood/bark	0.5
SCLEREID	Dicots leaves	0.63
CROSS	C_4 GSSCP	0.44
POLYLOBATE	C_4 GSSCP	0.27
POLYGONAL SCROBICULATE	Cyperaceae	0.21
ELONGATE SINUATE	Grass leaves/stems	0.15
SPHEROID ORNATE	Dicots wood/bark	0.14
SADDLE	C_4 GSSCP	0.11
ACUTE	Grass inflorescences	0.10
POLYGONAL	Dicots leaves	0.09
TRACHEARY	Dicots leaves	0.08
PLATELET	Dicots leaves	0.07
ELONGATE TUBERCULATE	Grasses inflorescences	0.05
IRREGULAR PSILATE	Dicots wood/bark	0.05
ACUTE BASE	Dicots leaves	0.01

Table S4. Phytolith morphotype frequencies by sample (see Excel file).

References

ANDERSEN, S.T. 1979. Identification of wild grass and cereal pollen. *Danmarks Geologiske Undersogelse* 17: 69–92.

ALBERT, R.M. & S. WEINER. 2001. Study of phytoliths in prehistoric ash layers from Kebara and Tabun caves using a quantitative approach, in J.D. Meunier, F. Colin & L. Faure-Denard (ed.) *Phytoliths: applications in earth science and human history*: 251–66. Lisse: Balkema.

ALBERT, R.M., J.A. RUÍZ & A. SANS. 2016. PhytCore ODB: a new tool to improve efficiency in the management and exchange of information on phytoliths. *Journal of Archaeological Science* 68: 98–105. https://doi.org/10.1016/j.jas.2015.10.014

ASCOUGH, P.L. *et al*. 2009. Hydropyrolysis as a new tool for radiocarbon pretreatment and the quantification of black carbon. *Quaternary Geochronology* 4: 140–47. https://doi.org/10.1016/j.quageo.2008.11.001

– 2020. Hydropyrolysis: implications for radiocarbon pretreatment and characterization of black carbon. *Radiocarbon* 52: 1336–50. https://doi.org/10.1017/S0033822200046427

BETTIS, E.A. 1984. New conventions for the designation of soil horizons and layers. *Plains Anthropologist* 29: 57–59. https://doi.org/10.1080/2052546.1984.11909221

BEUG, H.J. 2004. *Leitfaden der Pollenbestimmung fur Mittleuropa und angrenzende Gebiete*. Stuttgart: Fischer.

BROWN, A.G. *et al*. 2021. Ending the Cinderella status of terraces and lynchets in Europe: the geomorphology of agricultural terraces and implications for ecosystem services and climate adaptation. *Geomorphology* 379: 107579. https://doi.org/10.1016/j.geomorph.2020.107579

BROWN, D.A. 1984. Prospects and limits of a phytolith key for grasses in the central United States. *Journal of Archaeological Science* 11: 345–68. https://doi.org/10.1016/0305-4403(84)90016-5

DICKSON, C. 1988. Distinguishing cereal pollen from wild grass pollen: some limitations. *Circaea* 5: 67–71.

ELBAUM, R., S. WEINER, R.M. ALBERT & M. ELBAUM. 2003. Detection of burning of plant materials in the archaeological record by changes in the refractive indices of siliceous phytoliths. *Journal of Archaeological Science* 30: 217–26. https://doi.org/10.1006/jasc.2002.0828

Food and Agriculture Organization of the United Nations. 2006. *Guidelines for soil description* (Fourth edition). Rome: FAO Publications.

FAEGRI, K & J. IVERSEN. 1975. *Textbook of pollen analysis.* London: Blackwell Scientific.
FRAHM, E. 2017. First hands-on tests of an Olympus Vanta portable XRF analyzer to source Armenian obsidian artifacts. *International Association for Obsidian Studies Bulletin* 58: 8–23.
GOZUKARA, G. 2022. Rapid land use prediction via portable X-ray fluorescence (pXRF) data on the dried lakebed of Avlan Lake in Turkey. *Geoderma* 28: e00464.
GUR-ARIEH, S., E. MINTZ, E. BOARETTO & R. SHAHACK-GROSS. 2013. An ethnoarchaeological study of cooking installations in rural Uzbekistan: development of a new method for identification of fuel sources. *Journal of Archaeological Science* 40: 4331–47. https://doi.org/10.1016/j.jas.2013.06.001
HODGSON, J.M. 1976. *Soil survey field handbook* (Soil Survey Technical Monograph 5). Harpenden: Rothamsted Experimental Station.
International Committee for Phytolith Taxonomy. 2009. International Code for Phytolith Nomenclature (ICPN) 2.0. *Annals of Botany* 124: 189–99. https://doi.org/10.1093/aob/mcz064
KATZ, O. *et al*. 2010. Rapid phytolith extraction for analysis of phytolith concentrations and assemblages during an excavation: an application at Tell es-Safi/Gath, Israel. *Journal of Archaeological Science* 37: 1557–63. https://doi.org/10.1016/j.jas.2010.01.016
MCPARLAND, H. 2016. PhytoArkive project general report: phytolith assessment of samples from 16–22 Coppergate and 22 Piccadilly (ABC Cinema), York. Unpublished Insight Report, University of York.
MEREDITH, W. *et al*. 2012. Assessment of hydropyrolysis as a method for the quantification of black carbon using standard reference materials. *Geochimica et Cosmochimica Acta* 97: 131–47. https://doi.org/10.1016/j.gca.2012.08.037
MOORE, P.D., J.A. WEBB & M.E. COLLINSON. 1991. *Pollen analysis*. Oxford: Blackwell Scientific.
MULHOLLAND, S.C. & G. RAPP JR. 1992. A morphological classification of grass silica-bodies, in G. Rapp Jr & S.C Mulholland (ed.) *Phytolith systematics: emerging issues* (Advances in Archaeological and Museum Science 1): 65–89. New York: Springer. https://doi.org/10.1007/978-1-4899-1155-1_4
NEUMANN, K. *et al*. 2019. International Code for Phytolith Nomenclature (ICPN) 2.0. *Annals of Botany* 124: 189–99. https://doi.org/10.1093/aob/mcz064
PIPERNO, D. 2006. *Phytoliths: a comprehensive guide for archaeologists and paleoecologists*. Lanham (MD): Altamira.

REIMER, P.J. *et al*. 2020. The IntCal20 Northern Hemisphere radiocarbon age calibration curve (0–55 cal kBP). *Radiocarbon* 62: 725–57. https://doi.org/10.1017/RDC.2020.41

SANDERSON, D. & S. MURPHY. 2010. Using simple portable OSL measurements and laboratory characterization to help understand complex and heterogeneous sediment sequences for luminescence dating. *Quaternary Geochronology* 5: 299–305. https://doi.org/10.1016/j.quageo.2009.02.001

STUIVER, M., P.J. REIMER & R.W. REIMER 2022. *CALIB 8.2*. Available at: http://calib.org, (accessed 21 March 2022).

TWISS, P.C. 1992. Predicted world distribution of C_3 and C_4 grass phytoliths, in G. Rapp Jr & S.C Mulholland (ed.) *Phytolith systematics: emerging issues* (Advances in Archaeological and Museum Science 1): 113–28. New York: Springer. https://doi.org/10.1007/978-1-4899-1155-1_6

TWISS, P.C., E. SUESS & R.M. SMITH. 1969. Morphological classification of grass phytoliths. *Soil Science Society of America Journal* 33: 109–15. https://doi.org/10.2136/sssaj1969.03615995003300010030x

WADE, K., L-M, SHILLITO, J.M. MARSTON & C. BONSALL. 2019. Assessing the potential of phytolith analysis to investigate local environment and prehistoric plant resource use in temperate regions: a case study from Williamson's Moss, Cumbria, Britain. *Environmental Archaeology* 26: 295–308. https://doi.org/10.1080/14614103.2019.1619980

WEINER, S., P. GOLDBERG & O. BAR-YOSEF. 1993. Bone preservation in Kebara Cave, Israel using on-site Fourier transform infrared spectrometry. *Journal of Archaeological Science* 20: 613–27. https://doi.org/10.1006/jasc.1993.1037

ZHAO, P. *et al*. 2021. SOC stabilization mechanisms and temperature sensitivity in old terraced soils. *Biogeosciences* 18: 6301–12. https://doi.org/10.5194/bg-18-6301-2021

ZOHARY, D., M. HOPF & E. WEISS. 2012. *Domestication of plants in the Old World*. Oxford: Oxford University Press. https://doi.org/10.1093/acprof:osobl/9780199549061.001.0001